Published online 19 September 2016

Nucleic Acids Research, 2016, Vol. 44, No. 20 ***9591–9599***
doi: 10.1093/nar/gkw827

Global deformation facilitates flipping of damaged 8-oxo-guanine and guanine in DNA

Giuseppe La Rosa and Martin Zacharias*

Physik-Department T38, Technische Universität München, James-Franck-Straße 1, D-85748 Garching, Germany

Received June 16, 2016; Revised September 04, 2016; Accepted September 08, 2016

ABSTRACT

Oxidation of guanine (Gua) to form 7,8-dihydro-8-oxoguanine (8oxoG) is a frequent mutagenic DNA lesion. DNA repair glycosylases such as the bacterial MutM can effciently recognize and eliminate the 8oxoG damage by base excision. The base excision requires a 8oxoG looping out (flipping) from an intrahelical base paired to an extrahelical state where the damaged base is in the enzyme active site. It is still unclear how the damage is identified and flipped from an energetically stable stacked and paired state without any external energy source. Free energy simulations have been employed to study the flipping process for globally deformed DNA conformational states. DNA deformations were generated by systematically untwisting the DNA to mimic its conformation in repair enzyme encounter complex. The simulations indicate that global DNA untwisting deformation toward the enzyme bound form alone (without protein) significantly reduces the penalty for damage flipping to about half of the penalty observed in regular DNA. The finding offers a mechanistic explanation how binding free energy that is transformed to binding induced DNA deformation facilitates flipping and helps to rapidly detect a damaged base. It is likely of general relevance since repair enzyme binding frequently results in significant deformation of the target DNA.

INTRODUCTION

Oxidizing agents produced by cell metabolism, chemicals or ionizing radiation can lead to damage of DNA and associated diseases (1–3). One of the most frequent oxidative damages of DNA is the oxidation of guanine at position C8 yielding 7,8-dihydro-8-oxoguanine (8oxoG) (Figure 1A). If not repaired, 8oxoG can lead to a G:C to T:A transversion–mutation after subsequent replication rounds (4–7). Typically, DNA glycosylases (such as bacterial MutM and the human hOGG1 enzymes) can efficiently recognize the 8oxoG damage (among a surplus of 10^6–10^7 guanines) and eliminate the damaged base by the base excision and onset of subsequent repair processes (8–12).

Although the presence of the 8oxoG damage can lead to changes in the fine structure and dynamics of DNA (13–15) the overall structure of isolated 8oxoG containing duplex DNA is very similar to undamaged DNA. In addition, the thermal stability of 8oxoG–DNA is similar to regular duplex DNA of the same sequence (16–19). Initiation of the repair process requires flipping of the damaged base from an intrahelical based paired state toward an extrahelical (looped-out or flipped) conformation. The flipping process is energetically strongly disfavored since it involves disruption of Watson–Crick (WC) hydrogen bonds and unstacking of the damaged nucleo-base. Formation of the extrahelical state allows binding of the damaged base in the active site of the repair enzyme (e.g. MutM gylcosylase). Remarkably, the flipping and base excision by MutM and other glycosylases does not require additional energy in form of ATP or other chemical sources (10,12,20).

In order to identify a damaged site different mechanisms have been proposed. In a passive conformational selection mechanism the repair enzyme relies on a random base flipping event that leads to subsequent binding and initiation of the repair process. Given the low abundance of oxidized damaged guanine relative to undamaged DNA (e.g. in the order of 10^{-6}) the stability of the 8oxoG:C base pair further lowers the probability for forming an extrahelical conformation relative to the total concentration by a factor of 10^{-6}–10^{-7} according to estimates of the relative life times of the intrahelical and extrahelical states based on nuclear magnetic resonance (NMR) spectroscopy (21,22). Hence, in the passive recognition model, the effective concentration of accessible extrahelical damaged 8oxoG relative to undamaged bases at any given time point is only $\sim 10^{-12}$–10^{-13}. In contrast, during an active (induced fit) model, the repair enzyme binds first transiently forming an encounter complex (with the damaged site still in an intrahelical conformation) followed by the flipping process in the presence of the repair enzyme.

The latter mechanism is supported for the MutM repair enzyme but also other glycosylases by successful crystallization and structure determination of encounter complexes

*To whom correspondence should be addressed. Tel: +49 89 289 12335; Fax: +49 89 289 12444; Email: martin.zacharias@ph.tum.de

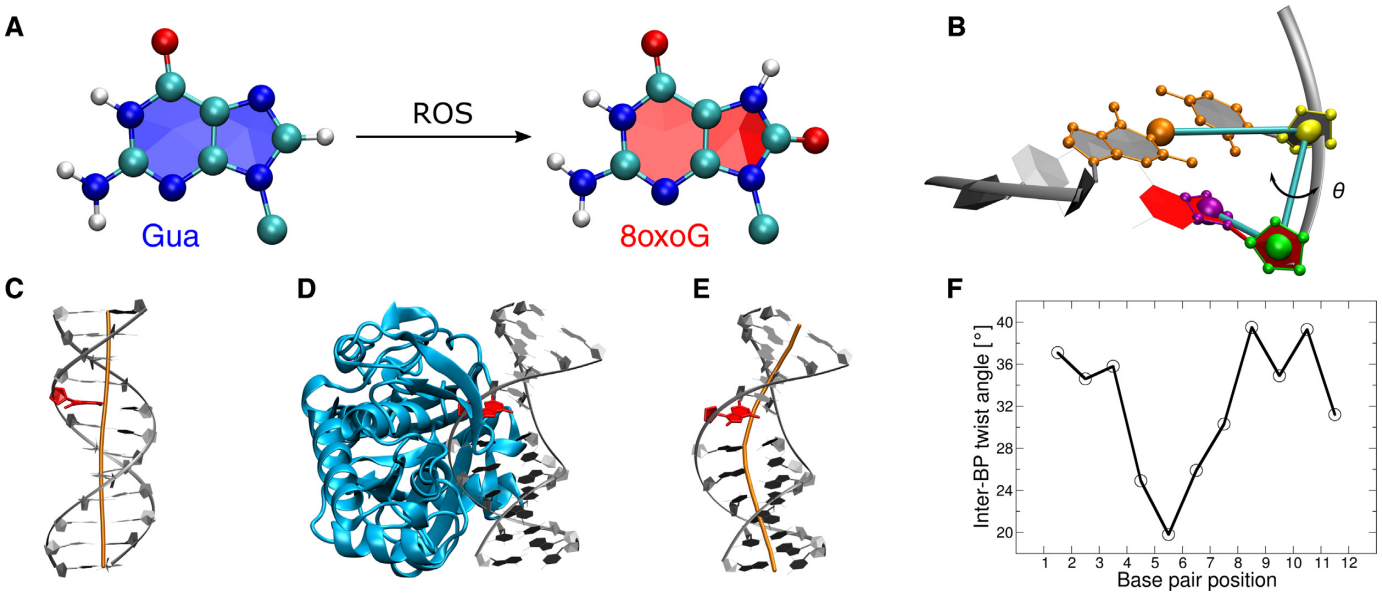

Figure 1. (**A**) 7,8-dihydro-8-oxoguanine (8oxoG) is the product of the interaction of reactive oxygen species (ROS) with guanine (Gua) nucleobase. Guanine is oxidized at position C8. (**B**) Generalized coordinate used for Hamiltonian replica exchange (H-REUS) simulations. The four centers of mass of four groups of atoms define the flipping pseudo dihedral angle (θ): (orange) the heavy atoms of the adjacent CG base pair 5′ to the flipping base, (yellow) the sugar moiety attached to the adjacent C 5′ of the target base, (green) the sugar attached to the target base and (purple) the purine five membered ring of the target base itself. Minor grove flipping is in the direction coming out of the page; major groove flipping is in the direction toward the the page. 8oxoG base is shown in red (other DNA bases and DNA backbone in gray). (**C**) B-DNA with a damaged 8oxoG (red) and straight helical axis (orange). (**D**) The repair enzyme (MutM gylcosylase, cyan cartoon) binds to the damaged DNA (grey) severely bending and locally untwisting the double helical structure [PDB ID: 3GO8]. (**E**) The DNA helical axis (orange) is bent in the enzyme bound damaged DNA (grey). (**F**) The plot represents the inter base pair twist angle as a function of the base pair position (8oxoG is at position 5) for the enzyme bound dsDNA.

with the damaged nucleotide in the intrahelical base-paired conformation (23,24). Nevertheless, still the next step of the recognition and repair process, a transition toward an extrahelical flipped state, may encounter a significant energy barrier.

Interestingly, most glycosylases including MutM severely bend and untwist DNA upon binding in order to associate with the DNA at the opened minor groove. This type of deformation occurs already in case of an encounter complex formation with the damaged base still in an intrahelical conformation (Figure 1C, D, E and F) (25–30).

Free energy simulations on flipping a damaged 8oxoG indicate that the presence of the protein but also DNA deformation facilitate the flipping process after an initial encounter binding (23,31,32). This is further supported by experimental studies indicating that negative DNA supercoiling (untwisting) can stimulate endonuclease and DNA repair activity (33).

In the present study, we specifically focus on the contribution of global DNA deformation to the flipping process. By employing global restraints on the twisting/bending of the DNA gradual global deformations of a DNA duplex containing a central 8oxoG are generated and the free energy of flipping has been calculated. In order to improve convergence of the free energy simulations, we use a combination of umbrella sampling and Hamiltonian replica exchange (H-REUS). For comparison, the corresponding free energy profiles of flipping an undamaged guanine nucleotide are also calculated.

The calculations indicate that global deformations such as local untwisting induced by the binding process of the repair enzyme result in a significant lowering of the penalty for base flipping. Hence, the induced fit process itself without direct contacts of the protein with the damaged DNA strongly facilitates the damage flipping. Such mechanism can dramatically accelerate the process of controlling the damaged state of a base pair by a repair enzyme. It also gives a mechanistic indication how the enzyme facilitates the thermodynamically unfavorable flipping process without requiring any external energy source such as ATP. It is likely that this mechanism is of general importance and may contribute also to other repair processes.

MATERIALS AND METHODS

Dodecamer duplex DNA molecules with sequences 5′-GTCCGGATCTAC-3′ (undamaged DNA) and 5′-GTCC(8oxoG)GATCTAC-3′ (damaged DNA) served as starting structures for molecular dynamics (MD) simulations (the sequences are the same as those in the crystal structure of the encounter complex with the MutM repair enzyme [PDB ID: 3GO8]) (23).

All MD simulations were carried out with the *pmemd* module of the Amber14 package using the *ff99-bsc0* force field including recent additional improvements for nucleic acids (34,35). All simulations were performed in explicit water (TIP3P) (36) with a truncated octahedral box and a minimum distance of 10 Å between DNA and box boundary. Potassium counter ions and chloride coions were included to neutralize the system and adjust to an ion concentration

of 125 mM. Potassium counter ions were used because they are present at higher concentration than sodium in the cell and nucleus. The simulation systems were first energy minimized (5000 steps) with positional restraints on DNA heavy atoms. The systems were then heated up in three stages (each stage 50 ps) to 300 k in steps of 100 K at a constant pressure of 1 bar (NPT ensamble) followed by gradual removal of the positional restraints from 25 kcal/(mol Å^2) to 0.5 kcal/(mol Å^2) (in 5 stages of 30 ps each) at constant volume (NVT ensamble). Before starting the umbrella sampling (US) simulations both systems were equilibrated for 10 ns at a temperature of 300 K and at constant volume without any restraints. Umbrella Sampling coupled with H-REUS simulations were performed to calculate the free energy profile for flipping a damaged or undamaged DNA base starting from the equilibrated structures containing either an 8oxoG or a regular G opposite to C. To enforce the flipping of the DNA target base we used a generalized coordinate similar to the one used by MacKerell *et al.* (37–42). The coordinate was defined by the pseudo dihedral angle (θ) formed by the centers of mass of four groups of atoms: (i) the heavy atoms of the adjacent CG base pair 5′ to the flipping base, (ii) the sugar moiety attached to the adjacent C 5′ of the target base, (iii) the sugar attached to the target base and (iv) the purine five membered ring of the target base itself (Figure 1B). The entire dihedral angle range from −177.5° to 180.0° was sampled in 2.5° steps (144 US windows). Every US window was sampled for 20 ns achieving an overall sampling time of about 2.8 μs for a single H-REUS run. The starting intrahelical base-paired configuration was defined by a pseudo dihedral angle of ∼40.0°. Decreasing the angle enforced the base to flip via the minor groove, while increasing it corresponded to major groove flipping (Figure 4A). Starting structures for every US window were generated using a quadratic penalty potential with a force constant of 10000 kcal/(mol Å^2). For subsequent production runs the force constant was lowered to 400 kcal/(mol Å^2). During the protocol a weak (5.0 kcal/(mol Å^2)) distance restraint between the centers of mass of the nearest and next-nearest neighbor base pairs was added to avoid undesired spontaneous flipping of neighboring bases during the simulations. This restraint was acting only in the case the distance of the centers of mass of the bases was greater than a threshold value of 6.5 Å. Potential of Mean Force (PMF) free energy profile for the flipping process were calculated using the weighted histogram analysis method (43–45). Uncertainties of the obtained PMFs were estimated by calculating the variance in the free energy estimator determined as the square of the cumulative statistical uncertainty as proposed by Zhu *et al.* (46). The variance on the PMF was computed from Equation 1 with the harmonic potential force constant k, the spacing of umbrella windows Δ_θ and the estimate of the mean position in the i-th window $\langle\theta_i\rangle$.

$$\mathrm{var}\big[G(\theta)\big] \approx (k\Delta_\theta)^2 \sum_{i=1}^{(\theta-\theta_0)/\Delta_\theta} \mathrm{var}[\langle\theta_i\rangle] \qquad (1)$$

The mean position in the i-th window $\langle\theta_i\rangle$ was estimated using the block averaging method (47).

Application of a torque on DNA base pairs upstream and downstream of the damaged base pair using another pseudo dihedral angle allowed a control of the mean twist per base pair of the DNA near the damaged site. The pseudo dihedral angle was defined by the centers of mass of four groups of atoms: (i) the sugar attached to the C base, two base pairs distant from the target base on 5′ direction, (ii) the sugar of the G base paired to the previous one on the opposite strand, (iii) the sugar of the A base, two base pairs distant from the target base on the 3′ direction and (iv) the sugar of the T base paired to the previous one on the opposite strand (Figure 2).

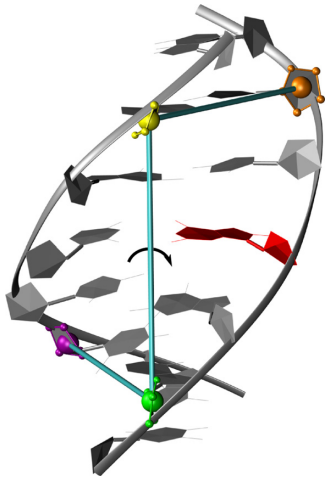

Figure 2. Localized DNA untwisting was obtained by applying a torque restraint on a pseudo dihedral angle defined by the centers of mass of four groups of atoms: (orange) the sugar attached to the C base, two base pairs distant from the target base on 5′ direction, (yellow) the sugar of the G base paired to the previous one on the opposite strand, (green) the sugar of the A base, two base pairs distant from the target base on the 3′ direction and (purple) the sugar of the T base paired to the previous one on the opposite strand. 8oxoG base is showed in red; other DNA bases and DNA backbone are showed in gray. Untwisting of the DNA and opening of the minor groove is obtained by clockwise rotation.

Average twist per base pair over the five base pairs affected by the torque restraint was calculated for standard B-DNA and for DNA in complex with the repair enzyme [PDB ID: 3GO8] resulting in ∼31°/bp and ∼27°/bp, respectively. The decrease of this value denotes an untwisting of the DNA caused by the action of the repair enzyme. This parameter is the one that will be used in the text as a measure of the untwisting level. To generate the starting structures for the H-REUS protocol the torque pseudo dihedral angle was restrained using a quadratic penalty potential (with a force constant of 400 kcal/(mol Å^2)) to four different decreasing values to produce gradually untwisting of the DNA. The corresponding average twist per base pair values that were obtained were approximately 32°/bp, 28°/bp, 26°/bp and 19°/bp (Figure 3). In correspondence of the decreasing twist per base pair an increase of the bending of the DNA axis can be noticed producing structures similar to the DNA in complex with the repair enzyme (compare Figure 3 with Figure 1E).

In addition to untwisting the DNA by an external torque US simulations were also performed with the heavy atoms of first and last three base pairs restrained to the positions of the corresponding bases of the DNA found in the encounter

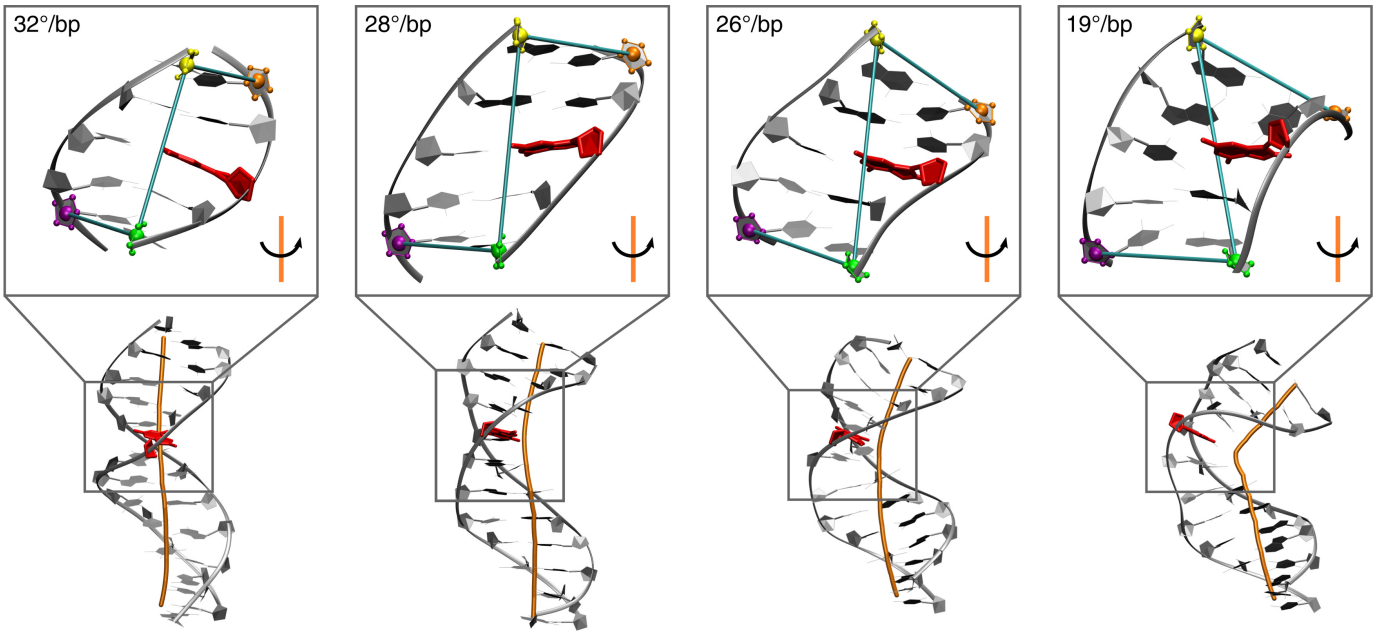

Figure 3. Equilibrated starting structures used for H-REUS in combination with local torque restraint. The local torque restraint (top) and the DNA axis bending (bottom) are highlighted. Untwisting level and consequent opening of the minor groove is directly proportional to an increase of the DNA bending. 8oxoG base is represented in red; DNA axis in orange; colored spheres and cyan sticks represent the torque restraint.

complex with the MutM repair enzyme [PDB ID: 3GO8] (23). Starting structures were generated using energy minimization and short MD simulations including positional restraints referenced to the corresponding coordinates of the DNA in the 3GO8 crystal structure.

Trajectories manipulation and data analysis were performed using the *cpptraj* module (48) of the AmberTools15 suite. DNA data, average parameters and DNA axis representation were elaborated using Curves+ (49).

RESULTS AND DISCUSSION

Nucleotide flipping in unrestrained B-DNA

Previous unrestrained MD simulations of dsDNA oligonucleotides with a central G:C or 8oxoG:C base pair indicated differences in the DNA fine structure but no spontaneous extrusion or flipping of the damaged guanine on the time scale (hundreds of ns) of current MD simulations (13). In order to compare the free energy required to flip a regular undamaged guanine and an oxidized 8oxoG umbrella sampling free energy simulations along a pseudo dihedral reaction coordinate were performed. The calculated profiles indicate a characteristic minimum around 40° of the reaction coordinate that corresponds to the intrahelical base paired state (Figure 4B). The H-REUS simulations predict an overall lower free energy penalty for flipping 8oxoG: ∼12.0 kcal/mol) compared to ∼14.0 kcal/mol in case of an undamaged G. The free energy curve is characterized by steep minimum with a near parabolic shape up to changes of ±15° from the optimum of the reaction coordinate. Interestingly, the transition to a near flat free energy surface occurs already a slightly smaller deviation from the free energy minimum along the reaction coordinate in case of 8oxoG versus undamaged G (especially for flipping along the minor groove, Figure 4B).

This difference can be explained by the formation of alternative hydrogen bonds in case of 8oxoG due to the two additional polar O8 and H7 atoms (Figure 4C). The flipping process toward the minor groove promotes formation of hydrogen bonds of these atoms with the opposing cytosine (C) which is not possible in case of guanine. In case of guanine flipping (at the same position along the reaction coordinate) instead the WC hydrogen are kept at the expense of a distorted conformation in order to keep the base pairing. The local distortions also lead to increased mobility but no spontaneous flipping of the opposing cytosine. Guanine is tilted into the DNA double helix causing also neighboring bases buckling (Figure 4C). The formation of additional contacts and the better solvation of the 8oxoG in the looped out solvent exposed state contribute to the lower free energy penalty for flipping the damaged versus undamaged guanine base. A small local minimum is visible at around −70.0° for both Gua and 8oxoG along the minor groove flipping path (more pronounced for 8oxoG). This minimum corresponds to a configuration where both bases are stacked into the DNA minor groove. In this state the damaged 8oxoG is aligned to the minor groove, while Gua points toward the groove resulting in a larger minor groove than in case of 8oxoG (Supplementary Data, Figure S1).

Proton exchange of the base polar hydrogens at the WC interface can be used to determine the equilibrium between intrahelical and extrahelical of damaged or undamaged bases (16,21,50–52). In order to define the onset of the transition we calculated the solvent accessibility (SASA) of the bases central polar hydrogen (H1) versus reaction coordinate. SASA was calculated using the 'rolling sphere' algo-

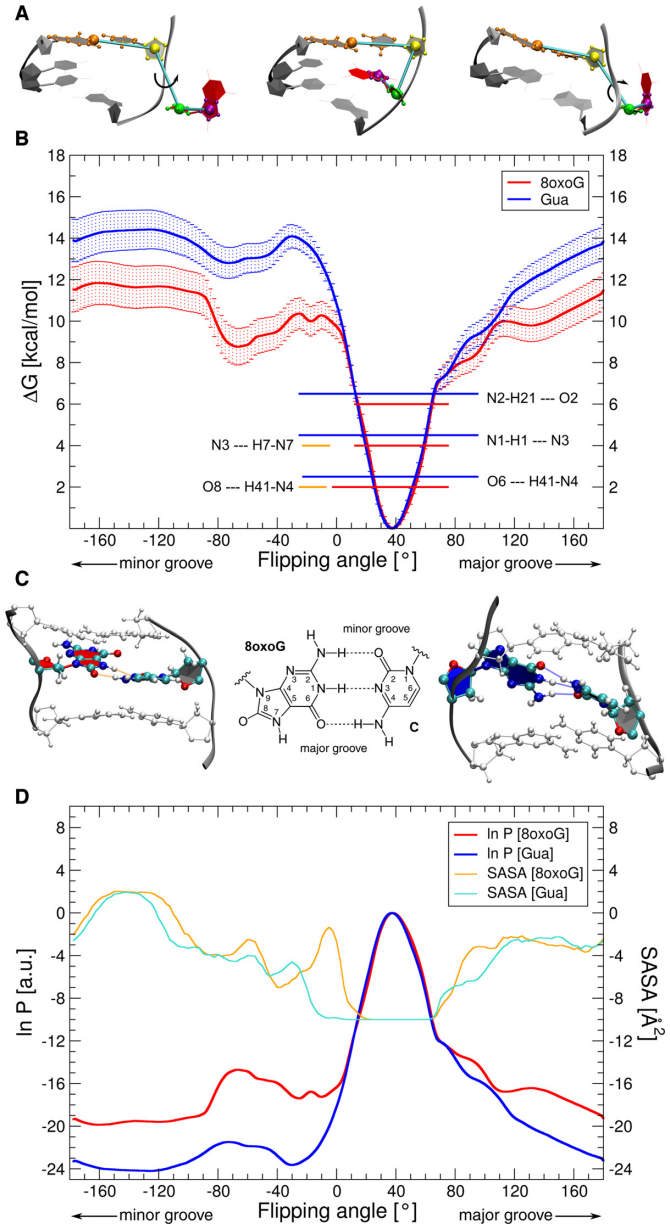

Figure 4. (**A**) Snapshots of flipped base (red) during umbrella sampling simulations (for clarity only the flipped base and neighboring base pairs are shown; pseudo centers are drawn as spheres with the defined flipping dihedral angle indicated as curved arrow; left and right panels indicate flipping toward the minor and major grooves, respectively, middle panel indicates the intrahelical state). (**B**) Calculated potential of mean force (PMF: free energy profile along the reaction coordinate) for flipping 8oxoG and G bases in normal B-DNA as a function of the defined flipping angle. Uncertainty of the calculated free energies are indicated as error bars (see Materials and Methods for details). Horizontal lines represent hydrogen bond formation among 8oxoG/G-C base pairs; blue and red lines represent the standard base pair hydrogen bonds, orange lines represent the two new hydrogen bonds formed only by 8oxoG while flipping toward the minor groove because of the presence of O8 and H7 atoms. (**C**) Snapshots of 8oxoG (left) and Gua (right) configurations at −17.5° flipping angle; hydrogen bonds are highlighted in orange for 8oxoG and in blue for G; the unperturbed Watson-Crick pairing is indicated in the middle panel. (**D**) Solvent accessible surface area (SASA) and logarithm of the flipping angle probability as a function of the flipping angle for 8oxoG and Gua flipping in B-DNA. SASA curves are shifted down by 10 Å^2.

rithm (53), with a probe radius of 1.4 Å that approximates the radius of a water molecule. We calculated the average SASA of the imino group N1-H1 (Figure 4C) of the 8oxoG or Gua base per US window and selected a threshold of 3.0 Å^2 (corresponding to the 25% of the maximum calculated SASA, i.e. 12 Å^2) to distinguish between intrahelical and extrahelical state (Figure 4D). The integration of the Boltzmann probability for the extrahelical regime and intrahelical regimes (obtained from the SASA calculations) allows the calculation of the equilibrium constant and the corresponding associated free energy (Table 1; this includes the entire range of looped out and intrahelical states).

The calculated free energies are in reasonable agreement with experiment except that experimentally 8oxoG was found to be slightly more stable than G in the intrahelical state. One should keep in mind that the experimental equilibrium between intrahelical and extrahelical states has been determined indirectly by proton exchange of the polar hydrogens and that some of the alternative hydrogen bonded states observed in our simulations (for 8oxoG) that we count as extrahelical may also contribute to reduced proton exchange in experiments in favor of an intrahelical state. Also, note that due to the exponential relation between free energy and equilibrium constant the differences between experimental and computational results are large when comparing equilibrium constants instead of free energy differences (Table 1).

Base flipping for twisted and bent B-DNA

The crystal structure of DNA in complex with repair enzymes (such as MutM) indicates significant global deformation and strong undertwisting of DNA and bending toward the major groove (opening of the minor groove). This is seen both in encounter complexes (with intrahelical damages) as well as complexes with a flipped base (27,28,30,54–56). To understand how the global deformation of the DNA influences the flipping process, we performed the same H-REUS protocol used above but including a restraint to deform the mean twist per base pair of the DNA near the damage site (Figure 3). The twist deformation was achieved by a quadratic penalty potential on a pseudo dihedral angle defined by four centers of mass on the next nearest base pairs upstream and downstream of the damaged base pair (see Materials and Methods for details). The effect of such restraint results in a local untwisting and bending of the DNA toward the major groove (Figure 3). The global shape of the DNA for the largest two twist deformations results in sampled structures that are similar to the shape of the DNA in the encounter complex with the MutM enzyme (compare Figure 3 and Figure 1E). The inclusion of the global deformation has a significant influence on the calculated PMF along the flipping coordinate (Figure 5).

Whereas restraining of the mean twist to the twist of regular B-DNA results in a slight increase of the flipping penalty (compared to flipping in unrestraint B-DNA, see Figure 4) the presence of a global untwisting deformation results in a decrease of the penalty which for the largest global deformation is almost half of the penalty observed for a global B-DNA shape (Figure 5). In addition, small shifts of the free energy minimum are observed. The free energy minimum

Table 1. Equilibrium constants and free energy differences for Gua and 8oxoG base flipping in B-DNA from simulation and experiment

		equilibrium constant ($\times 10^{-7}$)		ΔG_{op} (kcal/mol)	
flipping base	intrahelical range	calculated	experiment[a]	calculated	experiment[a]
Gua	−20.0°–77.5°	8.3 ± 7.8	3.1 ± 0.8	8.3 ± 0.5	8.8 ± 0.2
8oxoG	7.5°–77.5°	35.4 ± 40.8	2.1 ± 0.7	7.5 ± 0.6	9.1 ± 0.2

[a]Experimental values are taken from NMR imino proton exchange experiments (21).

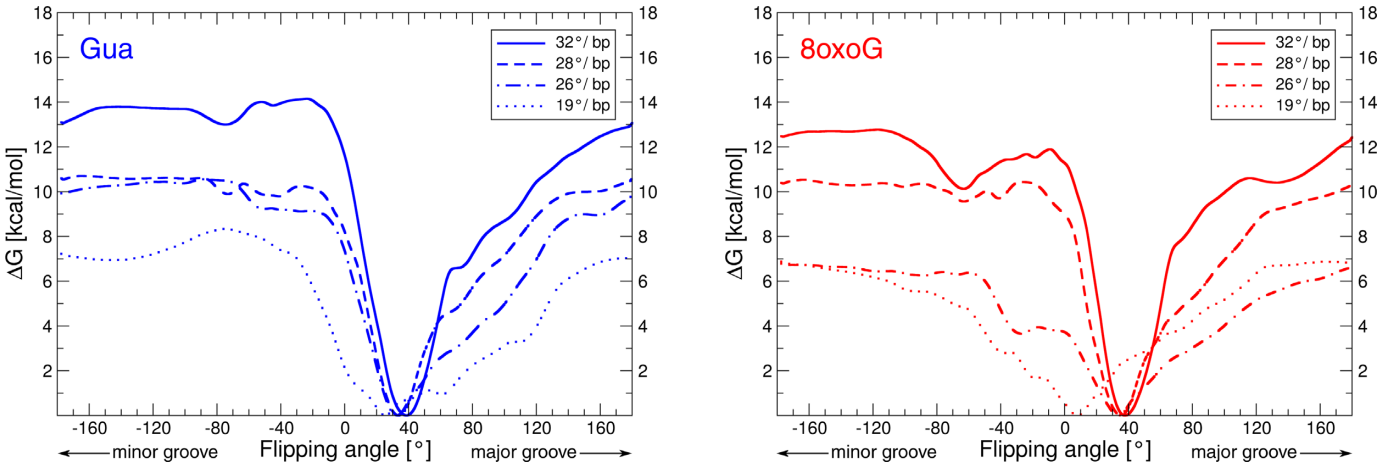

Figure 5. Potential of mean force (PMF: free energy profile along the reaction coordinate) for flipping Gua or 8oxoG as a function of the pseudo dihedral flipping angle and for different values of the local average twist angle restraint. Calculated uncertainties of the free energies are similar to the uncertainties obtained in the flipping simulation of B-DNA (Figure 4B), ∼±1.0 kcal/mol for the sampled extrahelical regime and ∼±0.5 kcal/mol in case of the intrahelical states and have been omitted for clarity.

funnel around the intrahelical state broadens especially for flipping toward the major groove.

In order to check if the lowering of the free energy penalty for flipping is due to the specific restraint applied to induce the global deformation we performed simulations with positional restraints on the heavy atoms of the three terminal base pairs at each end of the dsDNA molecules using the DNA in complex with the MutM repair enzyme (encounter complex) as reference structure (see Materials and Methods for details). Very similar to the free energy curves obtained for DNA deformed by an untwisting penalty the calculated flipping penalty for both a regular G and for the 8oxoG damage decreased significantly compared to B-DNA (Figure 6).

Integration of the Boltzmann probability for the intrahelical and extrahelical regimes along the reaction coordinate allows us to calculate the free energy of flipping versus twisting deformation of the DNA (Table 2 and Figure 7).

The result indicates that DNA deformation alone as observed in the encounter complex with MutM can considerably lower the penalty for damage flipping and besides of contacts with the protein contributes to the mechanism of rapid flipping without any external energy source like ATP.

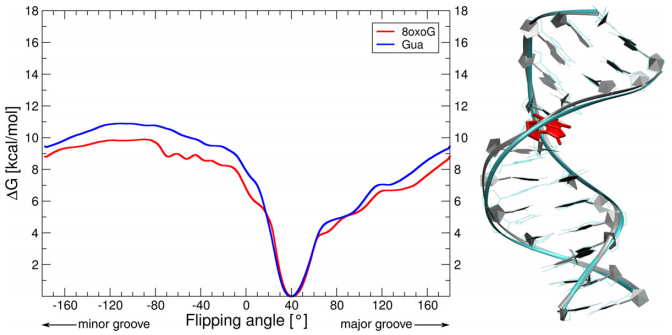

Figure 6. (left) Free energy PMF for flipping Gua and 8oxoG as a function of the pseudo dihedral flipping angle and for DNA restrained to the bent dsDNA found in complex with the repair enzyme (MutM). Calculated uncertainties of the free energies are similar to the uncertainties obtained in the flipping simulation of B-DNA (Figure 4B), ∼±1.0 kcal/mol for the sampled extrahelical regime and ∼±0.5 kcal/mol in case of the intrahelical states and and have been omitted for clarity. (right) Starting structure used to perform the H-REUS of bent DNA. Reference crystal structure is showed in cyan.

CONCLUSIONS

The application of H-REUS simulations allowed us to calculate the free energy profile for flipping damaged 8oxoG and for comparison also of regular guanine in the same sequence context. These simulations predicted a significant free energy penalty in good agreement with experiment and in qualitative agreement with previous simulations using different force fields, flipping restraints and sampling protocols (21,38–40,57–59).

In additional simulations global DNA deformation either in form of a gradual deformation or using the mean twist as deformation variable (which also results in bending and minor groove opening) or using restraints directly derived from the global DNA structure in the experimental encounter complex was included. In previous studies it

Table 2. Free energy differences for Gua and 8oxoG base flipping from simulations including an untwisting restraint on DNA.

	Gua		8oxoG	
avg twist/bp	intra. range	ΔG_{op}[a] (kcal/mol)	intra. range	ΔG_{op}[a] (kcal/mol)
32°	−17.5°–70.0°	6.8 ± 0.5 (7.4)	7.5°–77.5°	8.5 ± 0.4 (8.5)
28°	−10.0°–67.5°	4.9 ± 0.4 (5.8)	5.0°–92.5°	6.6 ± 0.6 (5.4)
26°	−10.0°–87.5°	4.5 ± 0.5 (3.8)	0.0°–57.5°	2.0 ± 0.3 (2.9)
19°	−27.5°–50.0°	0.9 ± 0.2 (2.4)	−7.5°–90.0°	1.5 ± 0.3 (2.1)

[a]Values in parenthesis are calculated considering the same intrahelical range for both Gua and 8oxoG, i.e. −20.0°–77.5°.

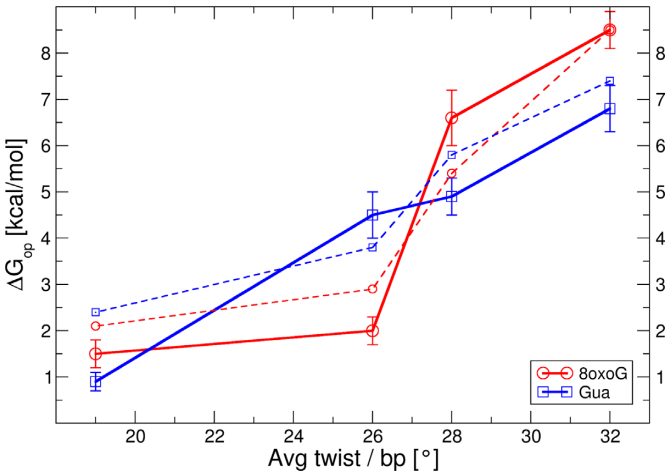

Figure 7. Calculated free energy of Gua and 8oxoG flipping as a function of the average twist angle generated by the applied torque restraint. A drastic drop in flipping free energy can be noticed in correspondence of a value of twist per base pair similar to the one exerted by the repair enzyme, i.e. ∼27°/bp. Dashed lines show the same free energy differences calculated considering the same intrahelical range for both Gua and 8oxoG, i.e. −20.0°–77.5°.

was found that the deformation of DNA as found in the encounter complex can result in a lowering of the free energy penalty for base flipping (23). However, the study started from the enzyme-bound conformation and included positional restraints to keep the DNA close to the deformed bound structure and this may stabilize both a specific local and global DNA conformation that results from the steric complementarity to the repair protein. For example, the enzyme bound structure is not only undertwisted but contains also a significant kink at the damaged base pair position (due to contacts with the protein) that may influence base flipping. In contrast, in the present study starting from B-DNA, specific twist deformations of different degrees were induced in a DNA molecule indicating a continuous lowering of the base flipping penalty correlated to the global twist deformation. As a control, we also performed simulations with positional restraints on the terminal base pairs steps to mimic a global deformation resembling the global structure of the DNA in the encounter complex which also showed a lowered penalty for flipping. Also these simulations were started from regular B-DNA and not the enzyme bound structure.

The simulations indicate that the global deformation of DNA upon binding alone facilitates the flipping process for both undamaged and damaged bases. In previous simulations we found that the presence of 8oxoG in DNA can result in local alterations of the backbone and sugar pucker fine structure (13,14). However, no significant differences in the helical deformability including twist deformability were observed (14). This is supported by experimental crystal structures of 8oxoG containing DNA that also indicate distinct changes in the nucleo-backbone structure compared to undamaged DNA. The altered fine structure likely modulates the initial encounter binding of damaged sites by repair enzymes. However, a major second effect is the induced deformation of DNA due to binding that facilitates the flipping process. Hence, binding energy is transformed to deformation energy of DNA which in turn lowers the penalty for flipping. The results of our study indicate that down to an untwisting of ∼27°/bp, ∼28°/bp the flipping of 8oxoG and Gua is facilitated to similar degrees and only at even lower twist values the penalty for 8oxoG flipping is lower than for flipping of Gua (Figure 7). It is possible that fluctuations of the DNA global deformation in the encounter complex can lead to transient further untwisting beyond the average ∼27°/bp observed in the X-ray structure that more specifically facilitates flipping of the 8oxoG damage. Alternatively, the distinction between a damaged 8oxoG and a Gua may occur at a later step along the repair pathway. This would imply that additional contacts with the repair protein, especially of the damaged base with protein atoms in the active site cleft, will further stabilize the looped out conformation and ultimately distinguish between a regular Gua or a damaged 8oxoG directly in the active site pocket. Since binding of repair enzymes frequently results in DNA distortion (especially undertwisting) it is likely that the present mechanism also plays a role in other repair processes. It gives a mechanistic explanation how protein–DNA binding free energy and associated DNA deformation can help to facilitate an energetically very costly flipping process from a stable intrahelical paired configuration to an extrahelical conformation.

ACKNOWLEDGEMENTS

The authors thank Dr A. Knips, F. Haese, F. Kandzia and F. Zeller for comments and fruitful discussions.

FUNDING

German Research Foundation (Deutsche Forschungsgemeinschaft) [SFB749, project C05]; Computer resources for this project have been provided by the Leibniz Supercomputing Centre (grant project pr48po). Funding for open access charge: Deutsche Forschungsgemeinschaft [SFB749, project C05].

Conflict of interest statement. None declared.

REFERENCES

1. Morreall,J.F., Petrova,L. and Doetsch,P.W. (2013) Transcriptional mutagenesis and its potential roles in the etiology of cancer and bacterial antibiotic resistance. *J. Cell. Physiol.*, **228**, 2257–2261.
2. Bjelland,S. and Seeberg,E. (2003) Mutagenicity, toxicity and repair of DNA base damage induced by oxidation. *Mutat. Res.*, **531**, 37–80.
3. Lindahl,T. (1993) Instability and decay of the primary structure of DNA. *Nature*, **362**, 709–715.
4. Neeley,W.L. and Essigmann,J.M. (2006) Mechanisms of formation, genotoxicity, and mutation of guanine oxidation products. *Chem. Res. Toxicol.*, **19**, 491–505.
5. Klaunig,J.E. and Kamendulis,L.M. (2004) The role of oxidative stress in carcinogenesis. *Annu. Rev. Pharmacol. Toxicol.*, **44**, 239–267.
6. Grollman,A.P. and Moriya,M. (1993) Mutagenesis by 8-oxoguanine: an enemy within. *Trends Genet.*, **9**, 246–249.
7. Shibutani,S., Takeshita,M. and Grollman,A.P. (1991) Insertion of specific bases during DNA synthesis past the oxidation-damaged base 8-oxodG. *Nature*, **349**, 431–434.
8. Prakash,A. and Doublié,S. (2015) Base excision repair in the mitochondria. *J. Cell. Biochem.*, **116**, 1490–1499.
9. Jacobs,A.L. and Schär,P. (2012) DNA glycosylases: In DNA repair and beyond. *Chromosoma*, **121**, 1–20.
10. Zharkov,D.O. (2008) Base excision DNA repair. *Cell. Mol. Life Sci.*, **65**, 1544–1565.
11. David,S.S., O'Shea,V.L. and Kundu,S. (2007) Base-excision repair of oxidative DNA damage. *Nature*, **447**, 941–950.
12. Fromme,J.C. and Verdine,G.L. (2004) Base excision repair. *Adv. Protein Chem.*, **69**, 1–41.
13. Kara,M. and Zacharias,M. (2013) Influence of 8-oxoguanosine on the fine structure of DNA studied with biasing-potential replica exchange simulations. *Biophys. J.*, **104**, 1089–1097.
14. Dršata,T., Kara,M., Zacharias,M. and Lankaš,F. (2013) Effect of 8-oxoguanine on DNA structure and deformability. *J. Phys. Chem. B*, **117**, 11617–11622.
15. Miller,J.H., Fan-Chiang,C.-C.P., Straatsma,T.P. and Kennedy,M.A. (2003) 8-Oxoguanine enhances bending of DNA that favors binding to glycosylases. *J. Am. Chem. Soc.*, **125**, 6331–6336.
16. Crenshaw,C.M., Wade,J.E., Arthanari,H., Frueh,D., Lane,B.F. and Núñez,M.E. (2011) Hidden in plain sight: subtle effects of the 8-oxoguanine lesion on the structure, dynamics, and thermodynamics of a 15-base pair oligodeoxynucleotide duplex. *Biochemistry*, **50**, 8463–8477.
17. Lipscomb,L.A., Peek,M.E., Morningstar,M.L., Verghis,S.M., Miller,E.M., Rich,A., Essigmann,J.M. and Williams,L.D. (1995) X-ray structure of a DNA decamer containing 7,8-dihydro-8-oxoguanine. *Proc. Natl. Acad. Sci. U.S.A.*, **92**, 719–723.
18. Plum,G.E., Grollman,A.P., Johnson,F. and Breslauer,K.J. (1995) Influence of the oxidatively damaged adduct 8-oxodeoxyguanosine on the conformation, energetics, and thermodynamic stability of a DNA duplex. *Biochemistry*, **34**, 16148–16160.
19. Oda,Y., Uesugi,S., Ikehara,M., Nishimura,S., Kawase,Y., Ishikawa,H., Inoue,H. and Ohtsuka,E. (1991) NMR studies of a DNA containing 8-hydroxydeoxyguanosine. *Nucleic Acids Res.*, **19**, 1407–1412.
20. Bruner,S.D., Norman,D.P. and Verdine,G.L. (2000) Structural basis for recognition and repair of the endogenous mutagen 8-oxoguanine in DNA. *Nature*, **403**, 859–866.
21. Every,A.E. and Russu,I.M. (2013) Opening dynamics of 8-oxoguanine in DNA. *J. Mol. Recognit.*, **26**, 175–180.
22. Leroy,J.L., Kochoyan,M., Huynh-Dinh,T. and Guéron,M. (1988) Characterization of base-pair opening in deoxynucleotide duplexes using catalyzed exchange of the imino proton. *J. Mol. Biol.*, **200**, 223–238.
23. Qi,Y., Spong,M.C., Nam,K., Banerjee,A., Jiralerspong,S., Karplus,M. and Verdine,G.L. (2009) Encounter and extrusion of an intrahelical lesion by a DNA repair enzyme. *Nature*, **462**, 762–766.
24. Banerjee,A., Santos,W.L. and Verdine,G.L. (2006) Structure of a DNA Glycosylase Searching for Lesions. *Science*, **311**, 1153–1157.
25. Velmurugu,Y., Chen,X., Slogoff Sevilla,P., Min,J.-H. and Ansari,A. (2016) Twist-open mechanism of DNA damage recognition by the Rad4/XPC nucleotide excision repair complex. *Proc. Natl. Acad. Sci. U.S.A.*, **113**, E2296–E2305.
26. Buechner,C.N., Maiti,A., Drohat,A.C. and Tessmer,I. (2015) Lesion search and recognition by thymine DNA glycosylase revealed by single molecule imaging. *Nucleic Acids Res.*, **43**, 2716–2729.
27. Koval,V.V., Knorre,D.G. and Fedorova,O.S. (2014) Structural features of the interaction between Human 8-Oxoguanine DNA glycosylase hOGG1 and DNA. *Acta Naturae*, **6**, 52–65.
28. Sung,R.-J., Zhang,M., Qi,Y. and Verdine,G.L. (2013) Structural and biochemical analysis of DNA helix invasion by the bacterial 8-oxoguanine DNA glycosylase MutM. *J. Biol. Chem.*, **288**, 10012–10023.
29. Rohs,R., Jin,X., West,S.M., Joshi,R., Honig,B. and Mann,R.S. (2010) Origins of specificity in protein-DNA recognition. *Annu. Rev. Biochem.*, **79**, 233–269.
30. Chen,L., Haushalter,K.A., Lieber,C.M. and Verdine,G.L. (2002) Direct visualization of a DNA glycosylase searching for damage. *Chem. Biol.*, **9**, 345–350.
31. Bergonzo,C., Campbell,A.J., De Los Santos,C., Grollman,A.P. and Simmerling,C. (2011) Energetic Preference of 8-oxodG Eversion Pathways in a DNA Glycosylase. *J. Am. Chem. Soc.*, **133**, 14504–14506.
32. Nam,K., Verdine,G.L. and Karplus,M. (2009) Analysis of an anomalous mutant of MutM DNA glycosylase leads to new insights into the catalytic mechanism. *J. Am. Chem. Soc.*, **131**, 18208–18209.
33. Collier,C., Machón,C., Briggs,G.S., Smits,W.K. and Soultanas,P. (2012) Untwisting of the DNA helix stimulates the endonuclease activity of Bacillus subtilis Nth at AP sites. *Nucleic Acids Res.*, **40**, 739–750.
34. Salomon-Ferrer,R., Case,D.A. and Walker,R.C. (2013) An overview of the Amber biomolecular simulation package. *WIREs Comput. Mol. Sci.*, **3**, 198–210.
35. Pérez,A., Marchán,I., Svozil,D., Sponer,J., Cheatham,T.E., Laughton,C.A. and Orozco,M. (2007) Refinement of the AMBER force field for nucleic acids: Improving the description of alpha/gamma conformers. *Biophys. J.*, **92**, 3817–3829.
36. Price,D.J. and Brooks,C.L. (2004) A modified TIP3P water potential for simulation with Ewald summation. *J. Chem. Phys.*, **121**, 10096–10103.
37. Song,K., Campbell,A.J., Bergonzo,C., de los Santos,C., Grollman,A.P. and Simmerling,C. (2009) An improved reaction coordinate for nucleic acid base flipping studies. *J. Chem. Theory Comput.*, **5**, 3105–3113.
38. Priyakumar,U.D. and MacKerell,A.D. (2006) Computational approaches for investigating base flipping in oligonucleotides. *Chem. Rev.*, **106**, 489–505.
39. Priyakumar,U.D. and MacKerell,A.D. (2006) NMR imino proton exchange experiments on duplex DNA primarily monitor the opening of purine bases. *J. Am. Chem. Soc.*, **128**, 678–679.
40. Banavali,N.K. and MacKerell,A.D. (2002) Free energy and structural pathways of base flipping in a DNA GCGC containing sequence. *J. Mol. Biol.*, **319**, 141–160.
41. Huang,N. and MacKerell,A.D. (2004) Atomistic view of base flipping in DNA. *Phil. Trans. A Math. Phys. Eng. Sci.*, **362**, 1439–1460.
42. Huang,N., Banavali,N.K. and MacKerell,A.D. (2003) Protein-facilitated base flipping in DNA by cytosine-5-methyltransferase. *Proc. Natl. Acad. Sci. U.S.A.*, **100**, 68–73.
43. Kumar,S., Rosenbergl,J.M., Bouzida,D., Swendsen,R.H. and Kollman,P.A. (1995) Multidimensional Free-Energy Calculations Using the Weighted Histogram Analysis Method. *J. Comput. Chem.*, **16**, 1339–1350.
44. Roux,B. (1995) The calculation of the potential of mean force using computer simulations. *Comput. Phys. Commun.*, **91**, 275–282.
45. Kumar,S., Bouzida,D., Swendsen,R.H., Kollman,P.A. and Rosenbergl,J.M. (1992) The weighted histogram analysis method for free-energy calculations on biomolecules. I. The method. *J. Comput. Chem.*, **13**, 1011–1021.
46. Zhu,F. and Hummer,G. (2012) Convergence and error estimation in free energy calculations using the weighted histogram analysis method. *J. Comput. Chem.*, **33**, 453–465.
47. Hess,B. (2002) Determining the shear viscosity of model liquids from molecular dynamics simulations. *J. Chem. Phys.*, **116**, 209–217.

48. Roe,D.R. and Cheatham III,T.E. (2013) PTRAJ and CPPTRAJ: Software for processing and analysis of molecular synamics trajectory data. *J. Chem. Theory Comput.*, **9**, 3084–3095.
49. Lavery,R., Moakher,M., Maddocks,J.H., Petkeviciute,D. and Zakrzewska,K. (2009) Conformational analysis of nucleic acids revisited: Curves+. *Nucleic Acids Res.*, **37**, 5917–5929.
50. Coman,D. and Russu,I.M. (2005) A nuclear magnetic resonance investigation of the energetics of basepair opening pathways in DNA. *Biophys. J.*, **89**, 3285–3292.
51. Várnai,P., Canalia,M. and Leroy,J.-L. (2004) Opening mechanism of G·T/U pairs in DNA and RNA duplexes: A combined study of imino proton exchange and molecular dynamics simulation. *J. Am. Chem. Soc.*, **126**, 14659–14667.
52. Chen,C. and Russu,I.M. (2004) Sequence-dependence of the energetics of opening of at basepairs in DNA. *Biophys. J.*, **87**, 2545–2551.
53. Shrake,A. and Rupley,J.A. (1973) Environment and exposure to solvent of protein atoms. Lysozyme and insulin. *J. Mol. Biol.*, **79**, 351–371.
54. Schneider,S., Schorr,S. and Carell,T. (2009) Crystal structure analysis of DNA lesion repair and tolerance mechanisms. *Curr. Opin. Struct. Biol.*, **19**, 87–95.
55. Hsu,G.W., Ober,M., Carell,T. and Beese,L.S. (2004) Error-prone replication of oxidatively damaged DNA by a high-fidelity DNA polymerase. *Nature*, **431**, 217–221.
56. Fromme,J.C. and Verdine,G.L. (2003) DNA lesion recognition by the bacterial repair enzyme MutM. *J. Biol. Chem.*, **278**, 51543–51548.
57. Giudice,E., Várnai,P. and Lavery,R. (2003) Base pair opening within B-DNA: Free energy pathways for GC and AT pairs from umbrella sampling simulations. *Nucleic Acids Res.*, **31**, 1434–1443.
58. Bernet,J., Zakrzewska,K. and Lavery,R. (1997) Modelling base pair opening : the role of helical twist. *J. Mol. Struct.*, **398**, 473–482.
59. Ramstein,J. and Lavery,R. (1988) Energetic coupling between DNA bending and base pair opening. *Proc. Natl. Acad. Sci. U.S.A.*, **85**, 7231–7235.